Dalton Trans

COMMUNICATION

Isomerisation, Reactivity and Coordination Chemistry of a New Hybrid, Multi-functional Phosphazane

Received 00th January 20xx,
Accepted 00th January 20xx

DOI: 10.1039/x0xx00000x

www.rsc.org/

Alex D. Plajer,[a] Kevin Bold,[a] Felix J. Rizzuto,[a] Raúl García-Rodríguez,*[,b] Tanya K. Ronson [a] and Dominic S. Wright*[,a]

The unsymmetric P^{III}/P^{V} cyclodiphosphazane framework [(S=)(H)P(μ-N^{t}Bu)$_2$PNH^{t}Bu] (2) provides entry into the mixed chalgogenide dianion [(S)P(μ-N^{t}Bu)$_2$P(Se)N^{t}Bu]$^{2-}$, and unique insight into the mechanisms of *cis*/*trans* isomerism in phosph(III)- and phosph(V)-azanes.

Establishing synthetic rules for the functionalisation and modification of ligand sets is a central subject in organic and inorganic chemistry. Adapting an established ligand allows easy control over the steric and electronic character in respect to coordination to metal centres. Much of our work has focused on the development of synthetic methodologies to inorganic ligand systems, which parallel developments in the organic arena. Phosph(III)azanes dimers have proved to be highly versatile building blocks in this area, being key starting materials for the construction not only of small multidentate ligand systems but also of large inorganic macrocycles. Highlighted in Figure 1 are two recent examples in which the phosphazane unit is used to construct *a)* a new type of hybrid carbene ligand,[1] and *b)* a large macrocyclic arrangement.[2,3]

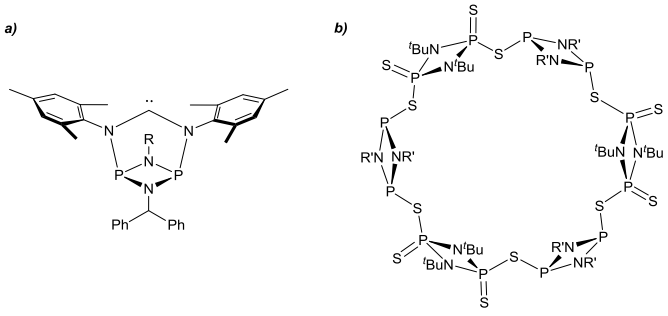

Figure 1 Examples of ligands derived from cyclodiphosphazane building blocks, a) a modified carbene ligand and b) a PIII/PV macrocycle.

One area of particular interest has been the uncovering of new synthetic methods for the selective donor-functionalisation of the P_2N_2 frameworks of cyclodiphosphazanes. A particularly important family in this class are the isoelectronic ligand systems shown in Figure 2, all of which can be readily accessed from nucleophilic substitution and/or oxidation of simple dichloro-phosphazanes [ClP(μ-NR)]$_2$ (e.g., Scheme 1).

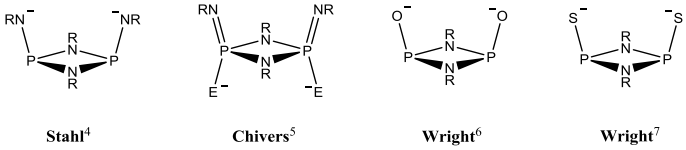

Figure 2 A series of isoelectronic multidentate dianionic ligands derived from nucleophilic substitution and/or oxidation of simple dicyclophosphazanes.

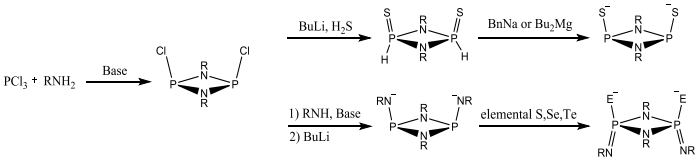

Scheme 1 Nucleophilic (top)[8] and oxidative (bottom)[9] functionalisation of a cyclodiphosphazane ring unit.

In the current study we set out with the simple aim of combining the previously established nucleophilic and oxidation reactions used in P_2N_2-functionalisation (illustrated in Scheme 1) to obtain the first examples of unsymmetric hybrid frameworks based on the diphosph(III/V)azane unit (Scheme 2). With these new arrangements in hand, we are able to observe direct evidence of the type of mechanism involved in *cis*/*trans* isomerisation (inter- or intra-molecular), as well as develop new ligand chemistry based on these multifunctional donor systems.

[a] *Chemistry Department, Cambridge University, Lensfield Road, Cambridge CB2 1EW (UK); e-mail dsw1000@cam.ac.uk.*
[b] *GIR MIOMeT-IU Cinquima-Química Inorgánica, Facultad de Ciencias, Campus Miguel, Delibes, Universidad de Valladolid 47011 Valladolid, Spain. e-mail raul.garcia.rodriguez@uva.es.*
[c] *Electronic Supplementary Information (ESI) available: Contains synthetic details, ^{1}H, ^{31}P, ^{77}Se NMR and X-ray analysis on all compounds. See DOI: 10.1039/x0xx00000x*

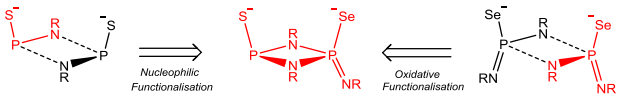

Scheme 2 Combining nucleophilic and oxidative functionalisation to produce hybrid ligands.

Synthetic studies started with the previously known unsymmetric cyclodiphosphazane [ClP(μ-N^{t}Bu)$_2$PNH^{t}Bu] (**1**), which can be conveniently prepared on a multigram scale by the reaction of PCl_3 with ^{t}BuNH$_2$ in 1 : 6 stoichiometric ratio (the excess ^{t}BuNH$_2$ acting as a Bronsted base to scavenge HCl). **1** was then reacted with a solution of LiSH in THF, prepared by the previously established procedure from the reaction of H_2S gas with ^{n}BuLi in THF.[8] *In situ* $^{31}P\{^1H\}$ spectroscopy showed complete conversion of **1** into the product [(S=)(H)P(μ-N^{t}Bu)$_2$PNH^{t}Bu] (**2**-*trans*) after 1 h at room temperature in THF, as indicated by the upfield shift of the P^{III} (P-Cl) resonance in **1** (d., δ = 201.2 ppm) to the P^V [P(H)(=S)] centre in **2**-*trans* (d., δ = 51.6 ppm, $^2J_{P\text{-}P}$ = 5.45 Hz), and the retention of the P^{III}-N(H)^{t}Bu group [δ = 136.1 ppm in **1**; cf δ = 130.0 ppm (br) in **2**-*trans*] (see ESI). In the fully-coupled ^{31}P NMR spectrum, the P^V [P(H)(=S)] resonance is observed as a double-doublet ($^2J_{PP}$ = 5.45 Hz, $^1J_{PH}$ = 531.5 Hz). Compound **2**-*trans* can be isolated as a crystalline solid in 63% yield after removal of the reaction solvent and crystallisation from toluene (see ESI). Further confirmation of the presence of a P-H proton and the retention of the N-H proton in **2**-*trans* comes from the ^1H NMR spectrum of the isolated material, with the P-H proton appearing as a double-doublet ($^1J_{P\text{-}H}$ = 531 Hz, $^2J_{P\text{-}P}$ = 9.8 Hz) and the N-H proton as a broad singlet (δ = 2.56 ppm) (see ESI).

Figure 3 shows that the solid-state structure of **2**-*trans* obtained under these conditions has a 'trans' arrangement, in which the ^{t}BuNH group and S atom are on opposite faces of the P_2N_2 ring unit. Noteworthy features of this arrangement are the disposition of the ^{t}BuNH group *exo* to the P_2N_2 ring fragment (presumably to avoid steric congestion with the μ-N^{t}Bu groups) and the planar conformation of the P_2N_2 ring.

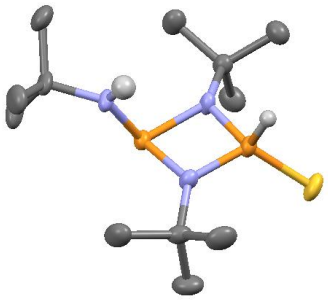

Figure 3 The structure of **2**-*trans*. H-atoms, except N-H and P-H, have been omitted for clarity. Thermal ellipsoids are drawn at the 50% probability level. Selected bond lengths (Å) and angles (°): P(1)-μ-N^{t}Bu range 1.648(3)-1.654(3), P(1)-S(1) 1.942(1), P(2)-μ-N^{t}Bu range 1.757(3)-1.761(3), P(2)-N(H)^{t}Bu 1.649(3), N^{t}Bu-P(1)-N^{t}Bu 85.4(1), N^{t}Bu-P(2)-N^{t}Bu 79.1(1), P(1)-μ-N^{t}Bu-P(2) range 97.4(1)-97.8(1).

Heating a sample of isolated **2**-*trans* to 50°C in THF for 16 h leads to complete conversion to **2**-*cis*. The isomerisation of **2** is signalled by the upfield shifts in the P^{III} and P^V $^{31}P\{^1H\}$ NMR resonances, to δ = 104.0 [d, $^2J_{P\text{-}P}$ = 11.1 Hz, P(III)] and 37.2 ppm (d, $^2J_{P\text{-}P}$ = 11.1 Hz, P(V)] in **2**-*cis*, from those in **2**-*trans* (δ = 130.0 and 51.6 ppm, respectively). **2**-*cis* can be crystallised from the reaction in 85% yield (see ESI). The solid-state structure is shown in Figure 4. The metric parameters in **2**-*trans* and **2**-*cis* are very similar. Significantly, there is little or no distortion of the P_2N_2 ring units of **2**-*trans* and **2**-*cis*, which are both almost planar. This can be compared to symmetric cyclo-diphosphazanes of the type [R'P(μ-NR)]$_2$, where the *trans* isomers have puckered ring units and the *cis* isomers have planar ring units.[4] To the best of our knowledge, there is only one other example in which the solid-state structures of both the *cis* and *trans* isomers of an individual cyclo-diphosphazane have been reported, [(PhCC)P(μ-N^{t}Bu)]$_2$.[10]

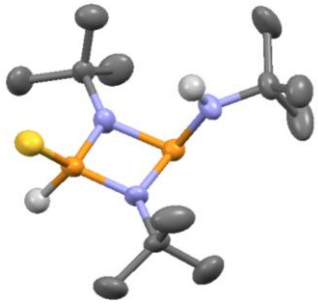

Figure 4 The structure of **2**-*cis*. H-atoms, except N-H and P-H, have been omitted for clarity. Only one of the two crystallographically-independent molecules is shown. Thermal ellipsoids are drawn at the 50% probability level. Selected bond lengths (Å) and angles (°): P^{III}-μ-N^{t}Bu range 1.650(5)-1.742(5), P^{III}-N(H)^{t}Bu range 1.638(6)-1.666(6), P^V-μ-N^{t}Bu range 1.645(6)-1.753(5),), P^V-S(1) range 1.918(2)-1.918(3), N^{t}Bu-P^{III}-N^{t}Bu range 79.0(3)-79.5(3), N^{t}Bu-P^V-N^{t}Bu range 84.8(3)-85.4(3), P^{III}-μ-N^{t}Bu-P^V range 97.5(3)-98.2(3).

Three potential isomerisation mechanisms have been proposed for cylclo-diphosphazanes: *(route a)* (vertex) lone-pair inversion at the P-centres, *(route b)* (edge) inversion at the bridging imido-N atoms, and *(route c)* cyclo-reversion followed by recombination (2+2 cycloaddition) of the monomer units.[4] While **2**-*trans* was too thermally unstable to investigate the kinetics of its *cis*/*trans* isomerisation further (prolonged heating in THF led to a complicated mixture of decomposition products), it is clear from the quantitative conversion of **2**-*trans* to **2**-*cis* in THF at 50°C that the process *cannot* involve intermolecular cyclo-reversion, otherwise the symmetrical phosphazane products would also be observed (Scheme 3).

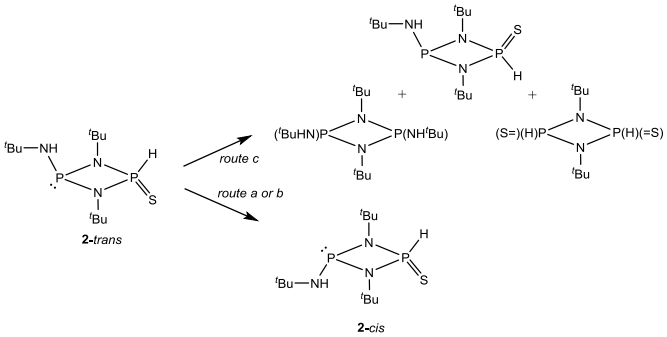

Scheme 3 Comparison of the products formed by (*route c*) intermolecular cyclo-reversion (top), and (*routes a or b*) intramolecular vertex or edge inversion (bottom).

The *in situ* $^{31}P\{^{1}H\}$ NMR spectrum of the reaction of **2**-*trans* with elemental selenium in toluene at room temperature consists of two doublets at δ = 36.2 [$^{2}J_{P\text{-}P}$ = 14.2 Hz, P(Se)] and 33.5 ppm [$^{2}J_{P\text{-}P}$ = 14.0 Hz, P(S)] (both splitting into a double-doublet in the fully-coupled spectrum) (see ESI). This product, [(S=)(H)P(μ-N^{t}Bu)$_2$P(=Se)NH^{t}Bu] (**3a**), can be isolated as a powder in 94% yield after filtration and removal of the solvent under vacuum (see ESI). The ^{77}Se NMR spectrum of isolated **3a** in $CDCl_3$ shows a doublet ($^{1}J_{P\text{-}Se}$ = 560.6 Hz), consistent with the oxidation of **2**-*trans* at its P^{III} centre (see ESI). The solid-state structure of **3a** shows that the oxidation of **2**-*trans* is stereoselective, with retention of the *trans*-configuration of the ^{t}BuN(H)-group and S-atom (Figure 5). Like **2**-*cis and* **2**-*trans*, the P_2N_2 ring unit in **3a** is almost completely planar; however, an interesting difference is found in the *endo*-orientation of the ^{t}BuNH-group with respect to the P_2N_2 ring (cf. the *exo* disposition in **2**-*trans* and **2**-*cis*). Since there are no intermolecular N-H···S or ···Se interactions occurring in the lattice, it appears that this is due to the steric influence of the Se atom now bonded to the P-centre.

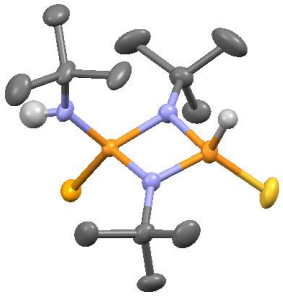

Figure 5 The structure of **3a**. H-atoms, except N-H and P-H, have been omitted for clarity. Only one of the two independent molecules is shown. Thermal ellipsoids are drawn at the 50% probability level. Selected bond lengths (Å) and angles (°): P_S-μ-N^{t}Bu range 1.674(4)-1.678(4), P_S-S 1.926(2)-1.930(2), P_S-μ-N^{t}Bu range 1.685(4)-1.698(3), P_{Se}-N(H)^{t}Bu 1.627(4)-1.630(4), P_{Se}-Se 2.090(1)-2.099(1), N^{t}Bu-P-N^{t}Bu 83.0(2)-84.2(2), P_{Se}-μ-N^{t}Bu-P_S range 95.8(2)-96.3(2). The P and N atoms of the P_2N_2 ring unit are only deviated *ca.* 5.7° out of the plane.

Unlike **2**, **3a** is thermally stable in solution for prolonged periods, allowing the investigation of its isomerisation. Figure 6 shows the changes observed in the $^{31}P\{^{1}H\}$ NMR spectrum of **3a** upon heating a sample in d_8-toluene over the temperature range 40-90 °C. Heating to 40 °C for 24 h results in the appearance of two new resonances at δ = 29.7 [d, $^{2}J_{PP}$ = 9.8 Hz, P(Se)] and 22.9 ppm [d, $^{2}J_{PP}$ = 8.4 Hz, P(S)] [cf. **3a** δ = 36.2 (d, $^{2}J_{P\text{-}P}$ = 14.2 Hz, P(Se)), 33.5 ppm (d, P(S), $^{2}J_{P\text{-}P}$ = 14.0 Hz)]. The $^{31}P\{^{1}H\}$ chemical shift in **3b** is similar to that reported for *cis*-[^{t}BuNH)(Se)P(μ-N^{t}Bu)]$_2$ (δ = 26.7 ppm).[9a] Additional information comes from the ^{1}H NMR spectrum of the solid reaction products in $CDCl_3$ recovered after 3 h at 60 °C, which shows the appearance of a new set of P-H, N-H and ^{t}Bu resonances in the same relative ratio as that found in **3a**, identifying this species (**3b**) as an isomer of **3a**, with the S and Se atoms *trans* rather than *cis* with respect to the P_2N_2 ring unit (Scheme 4) (see ESI). The $^{31}P\{^{1}H\}$ NMR spectrum of the reaction of solid Se with the **2**-*cis* in toluene also shows the formation of **3b**. However, unlike the reaction of **2**-*trans* with Se which occurs smoothly at room temperature, a complicated mixture of products is produced at the higher reaction temperature required (at reflux).

In addition to the resonances for **3b**, a further singlet resonance is also apparent after 24 h at 40 °C (δ = 30.8 ppm). Further heating of the reaction to 90 °C for 7 days results in the exclusive formation of this species, the consumption of **3a** and **3b** and the precipitation of a white solid. The new species was identified as the previously reported symmetric cyclodiphosphazane [(^{t}BuNH)(Se)P(μ-N^{t}Bu)]$_2$ (**4**) (Scheme 4) on the basis of spectroscopic analysis (lit. $^{31}P\{^{1}H\}$ NMR δ = 26.7 ppm in THF) (see ESI).[9a] The formation of **4** supports the view that the isomerisation of **3a** to **3b** occurs (at least in part) by the intermolecular cyclo-reversion mechanism. Since the other product of this reaction, symmetric [(S=)(H)P(μ-N^{t}Bu)]$_2$ (**5**) (Scheme 4), is known to be thermally unstable,[8] it is not surprising that this component is not observed in the final NMR spectrum (and is presumably the source of the white solid decomposition product).

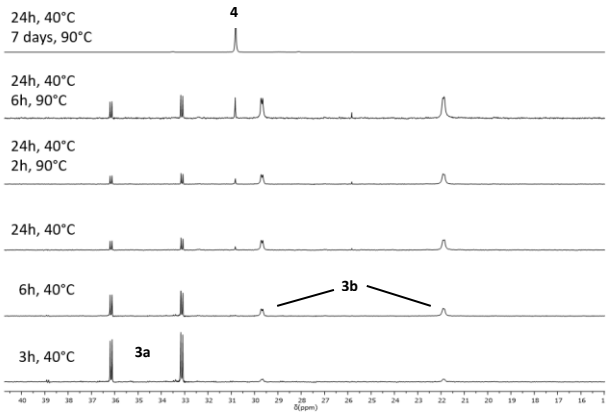

Figure 6 The development of the *in situ* $^{31}P\{^{1}H\}$ NMR spectrum of **3a** with time at 40-90 °C in d_8-toluene.

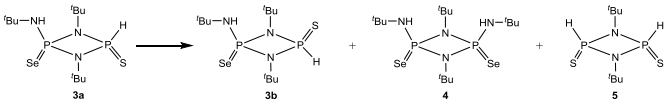

Scheme 4 The thermal isomerism of **3a** to **3b**, with the formation of other potential products resulting from cyclo-reversion.

The kinetics of the conversion of **3a** to **3b** was followed by further NMR experiments. The relative integrals of the P-H proton resonances were measured at a temperature of 50 °C for a total time of 588 mins, with NMR spectra being recorded every six mins (a total of 99 separate measurements). As can be seen from Figure 7, the isomerisation of **3a** to **3b** follows first-order kinetics (with R^2 = 0.994). Our overall conclusion, drawn from these data and that shown in Figure 6, is that the isomerisation of **3a** to **3b** is probably largely *via* cyclo-reversion, in which the dissociation of **3a** into two monomer units is rate determining. We cannot, however, exclude a contribution from intramolecular mechanisms (especially at lower temperatures).

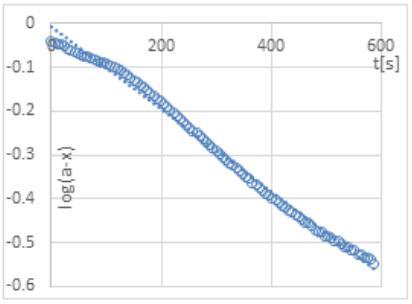

Figure 7 Graph of the log of the concentration of **3a** [(a-x) mol^{-1}] at time (t). The straight line is the best fit line, with $R^2 = 0.994$.

3a is readily deprotonated at both the N-H and P-H positions by reaction with benzylsodium (2 equiv.) in THF at room temperature. The Na complex $[Na(THF)Na(THF)_{2.5}\{(S)P(\mu\text{-}N^tBu)_2P(Se)N^tBu\}]$ (**6**) can be isolated in crystalline form after layering the reaction with *n*-hexane (in 24% yield) (see ESI). A polymeric arrangement is found for **6** in the solid state (Figure 8), in which the $[(S)P(\mu\text{-}N^tBu)_2P(Se)N^tBu]^{2-}$ dianion units are held together by alternating *mono*-THF solvated (four-coordinate) Na^+ cations [Na(1)] by side-on N/Se- and S-bonding on either side of the dianion. The other Na^+ cation [Na(2)] is solvated by three THF ligands, with one of the THF ligands disordered over coordinated and non-coordinated sites (*ca.* 50:50). This Na^+ cation is chelated by the S and Se atoms of the dianion (resulting in trigonal bipyramidal geometry). The large reduction in the *exo*-^{t}BuN-P [P(2)-N(3) 1.574(4) Å] bond length compared to that in **3a** [cf. *ca.* 1.63 Å] reflects the increase in Zwitter-ionic character upon deprotonation. The retention of the original conformation of the ^{t}BuN-group and S- and Se-atoms upon deprotonation of **3a** at room temperature is a particularly noteworthy feature of **6**. Consistent with this conformational rigidity, if a mixture of isomers **3a** and **3b** (2 : 1) is deprotonated with benzylsodium in THF both the *cis*- and the *trans*-$[(S)P(\mu\text{-}N^tBu)_2P(Se)N^tBu]^{2-}$ dianions are observed in solution (in the same 2 : 1 ratio as the starting materials).

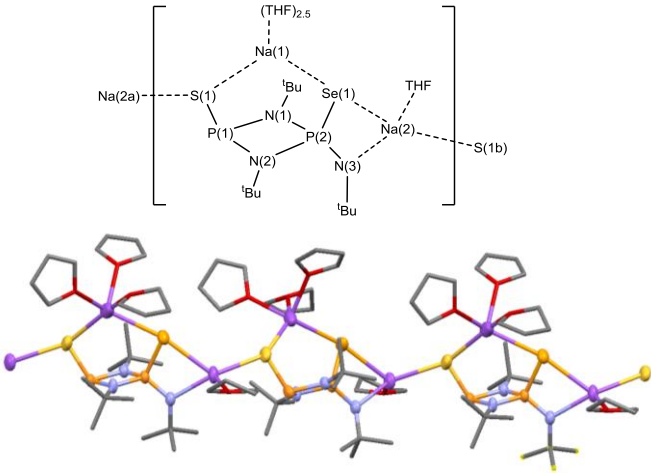

Figure 8 a) Connectivity and numbering scheme, and b) polymeric arrangement of **6**. H-atoms have been omitted for clarity. The diagram shows all of the three THF ligand environments attached to Na(2), one of which is disordered over two 50:50 sites with the O-atom pointing towards the Na^+ cation and one THF environment in which the O-atom points away from the Na^+ cation (see ESI). Thermal ellipsoids are drawn at the 50% probability level for the heavy atoms, the THF ligands have been drawn as wire frames. Selected bond lengths (Å) and angles (°): P(1)-N(1) 1.751(4), P(1)-N(2) 1.746(3), P(1)-S(1) 2.068(2), P(2)-N(1) 1.693(3), P(2)-N(2) 1.680(3), P(2)-N(3) 1.574(4), P(2)-Se(1) 2.187(1), Na(1)-S(1) 2.761(3), Na(1)-Se(1) 2.894(2), Na(2)-Se(1) 2.924(2), Na(2)-N(3) 2.374(4), Na(2a)-S(1) 2.790(2), P(1)-μ-N^{t}Bu-P(2) 98.4(2)-99.2(2), N(1)-P(1,2)-N(2) 79.4(2)-83.0(2), Se(1)-P(2)-N(3) 105.7(1).

In conclusion, by combining previously established synthetic approaches we have been able to build an unsymmetrical P^{III}/P^V cyclo-phosphazane framework, $[(S=)(H)P(\mu\text{-}N^tBu)_2PNH^tBu]$ (**2**). Both the *cis* and *trans* isomers of **2** have been structurally characterised, with the thermally-activated *cis*/*trans* isomerisation following an intramolecular pathway. Further elaboration of this framework by oxidation of the P^{III} centre with Se gives the new P^V species $[(S=)(H)P(\mu\text{-}N^tBu)_2P(=Se)NH^tBu]$ (**4**), which also undergoes *cis*/*trans* isomerism in this case largely *via* a dissociative cyclo-reversion mechanism. Deprotonation of **4** gives the $[(S)P(\mu\text{-}N^tBu)_2P(Se)N^tBu]^{2-}$ dianion, the sodium salt of which is a potential starting material for transmetallation reactions with other main group and transition metals.

Acknowledgements We thank the EU (ERA Advanced Grant for DSW, Erasmus Programme KB), Cambridge Australia Scholarships and the Cambridge Trust (FJR), for funding and the Spanish MINECO-AEI and the European Union (ESF) for a Ramon y Cajal contract (RG-R, RYC-2015–19035).

Notes and references

1 T. Roth, V. Vasilenko, C. G. M. Benson, H. Wadepohl, D. S. Wright, L. H. Gade, *Chem Sci*., 2015, **6**, 2506.
2 A. J. Plajer, R. García-Rodríguez, C. G. M. Benson, P. D. Matthews, A. D. Bond, S. Singh, L. H. Gade, D. S. Wright, *Angew. Chem. Int. Ed*., 2017, ***56***, *9087*.
3 See also, T. Roth, H. Wadepohl, D. S. Wright, L. H. Gade, *Chem Eur. J*., 2013, **19**, 13823; S. Gonzalez Calera and D. S. Wright, *Dalton Trans*., 2010, **39**, 5055.
4 L. Stahl, *Coord. Chem. Rev*., 2000, **210**, 203; M. S. Balakrishna, D. J. Eisler, T. Chivers, *Chem. Soc. Rev*., 2007, **36**, 650; M. S. Balakrishna, *Dalton Trans*., 2016, **45**, 12252.
5 R. Davies, L. Patel, *Chalcogen-Phosphorus (and Heavier Congener) Compounds: Handbook of Chalcogen Chemistry: New Perspectives in Sulfur, Selenium and Tellurium*, 2nd ed.; Devillanova, F. A.; du Mont, W-W., Eds.; RSC Publishing: UK, 2013; Vol. 1, Chapter 5, pp 238; A. Nordheider, J. D. Woolins, T. Chivers, *Chem. Rev*., 2015, **115**, 10378.
6 W. T. K. Chan, F. García, S. Gonzalez-Calera, M. McPartlin, J. V. Morey, R. E. Mulvey, S. Singh, D. S. Wright, *Chem. Commun*., 2008, 2251.
7 C. G. H. Benson, A. Plajer, R. García-Rodríguez, A. D. Bond, S. Singh, L. H. Gade, D. S. Wright, *Chem. Commun*., 2016, **52**, 9683.
8 C. G. M. Benson, V. Vasilenko, R. García-Rodríguez, A. D. Bond, S. G. Calera, L. H. Gade, D. S. Wright, *Dalton Trans*., 2015, **44**, 14242
9 (a) T. Chivers, M. Krahn, M. Parvez, *Chem. Commun*., 2000, 463; (b) T. Chivers, M. Krahn, M. Parvez, G. Schatte, *Inorg. Chem*., 2001, **40**, 2547.
10 M. M. Siddiqui, J. T. Mague, M. S. Balaskrishna, *Inorg. Chem*., 2015, **54**, 1200.

